

# Polarizabilities of Platonic Solids

Ari Sihvola, *Senior Member, IEEE*, Pasi Ylä-Oijala, Seppo Järvenpää, and Juha Avelin

**Abstract**—This article presents results of a numerical effort to determine the dielectric polarizabilities of the five regular polyhedra: tetrahedron, cube, octahedron, dodecahedron, and icosahedron. The polarizability is calculated by solving a surface integral equation, in which the unknown potential is expanded using third-order basis functions. The resulting polarizabilities are accurate to the order of  $10^{-4}$ . Approximation formulas are given for the polarizabilities as functions of permittivity. Among other results, it is found that the polarizability of a regular polyhedron correlates more strongly with the number of edges than with the number of faces, vertices, or the solid angle seen from a vertex.

**Index Terms**—High-order basis functions, polarizability, polyhedra, surface integral equation.

## I. INTRODUCTION

WHEN a dielectric inclusion is put into a homogeneous electric field, it causes a perturbation to the total electric field distribution. The perturbation is concentrated in the neighborhood of the inclusion. In connection with this problem in electrostatics, the concept of polarizability of such an inclusion is important. The main component of the “scattered field,” in other words the difference between the total field when the scatterer is present and the uniform incident field, is a dipolar field. This electrostatic dipolar field (which decays according to the inverse cube of the distance from the scatterer) can be identified as arising from a point dipole. Subsequently, the polarizability is the ratio between the dipole moment and the amplitude of the incident field.

The present article focuses on the numerical calculation of the polarizability of inclusions whose shape does not allow an analytical solution for the electrostatic problem.

In terms of a formal relation, the polarizability  $\alpha$  is defined by

$$\mathbf{p} = \alpha \mathbf{E}_e \quad (1)$$

where  $\mathbf{E}_e$  is the uniform external field and  $\mathbf{p}$  the induced dipole moment. In this equation, the polarizability is assumed to be equivalent to scalar, meaning that the dipole is parallel to the external field. Such is the case in the analysis to follow, but it is important to bear in mind that this is a special case. If we have an anisotropic inclusion, usually the polarizability is a dyadic. This happens also in the case if the external shape or internal structure of the scatterer are nonsymmetric or otherwise complicated.

A simple example of an isotropic scatterer is a homogeneous sphere. If the sphere has permittivity  $\epsilon_i$ , and it is embedded in an environment with permittivity  $\epsilon_e$ , the polarizability is well known [1]:

$$\alpha = 3\epsilon_e V \frac{\epsilon_i - \epsilon_e}{\epsilon_i + 2\epsilon_e} \quad (2)$$

Manuscript received November 21, 2002; revised December 9, 2003.

The authors are with the Electromagnetics Laboratory, Helsinki University of Technology, Espoo 02015, Finland (e-mail: ari@eml.hut.fi).

Digital Object Identifier 10.1109/TAP.2004.834081

where  $V$  is the volume of the sphere. A closed-form result arises from the solution of the Laplace equation in the geometry, and is easy to derive because the internal field is uniform for a spherical geometry. Although polarizability is a static concept it can also be used in problems involving time-dependent fields if the size of the scatterer is much smaller than the wavelength of the field.

But save for ellipsoids whose static response can be represented in terms of the depolarization factors [2], inclusions shaped otherwise do not generally have a closed-form expression for the polarizability. To analyze more complex shapes, numerical efforts are needed. In this work, the intention is to give accurate results for the electrostatic polarizabilities of regular polyhedra, also called as Platonic solids. As mentioned, for these scatterers, the problem cannot be solved in closed form, even if they are homogeneous in structure.

There are five regular polyhedra: tetrahedron, hexahedron (cube), octahedron, dodecahedron, and icosahedron. A regular polyhedron is a solid, three-dimensional (3-D) figure each face of which is a regular polygon with equal sides and equal angles. Also, its vertices are equal. These Platonic polyhedra (with the number of faces 4, 6, 8, 12, 20, respectively) are fundamental shapes like a sphere. In electrostatics, they can be described by very few parameters: the volume and the dielectric permittivity.

Earlier work exists on the electrostatic analysis of dielectric cubes and other rectangular polyhedra. Already in 1961, Edwards and Van Bladel [3] solved numerically the integral equation for the potential on the surface of a dielectric cube in a case where it is placed in uniform field. Reasonable estimates for the polarizability of the cube were calculated in the end of 1970's by Herrick and Senior [4], and also by Eyges and Gianino [5]. In light of the present results, these evaluations were correct to the order of a few per cent. In recent years, the cube and also some other polyhedra have been studied with more powerful computers and numerical schemes as these early results. Avelin *et al.* [6], [7] have published approximate formulas from which the polarizability of a cube, tetrahedron, and octahedron can be evaluated with inaccuracy below one per mille. Another important series of results has been published by Mansfield *et al.* [8] where a Monte Carlo-type random walk approach is applied to the potential problem of heat conduction. Among the results of their paper, the limiting values (when the permittivity approaches infinity) for the polarizabilities of polyhedra are given.

In addition to polarizability calculations, there are studies [9]–[12] in which the aim is to calculate the effective properties of structures with cube-shaped and other particles. The effective permittivity (or conductivity) of such a mixture is connected to the polarizability amplitude of a single scatterer. The polarizability is proportional to the slope of the effective permittivity curve when the volume fraction of the inclusion phase in the mixture is very small (the first term of the Taylor expansion).

In the following, our aim is to present calculations to a very high accuracy of the polarizabilities of all five Platonic solids, that are dielectrically homogeneous, for all possible permittivity values between zero and infinity, and also to evaluate the accuracy of these earlier results. In addition, approximate formulas will be given for the polarizability as functions of permittivity.

Calculation of the polarizabilities is based on a surface integral equation formulation for the static potential. In the previous calculations [6], [7] the potential was expressed by piecewise constant basis functions. To have a more powerful and accurate representation for the potential, in this paper higher order basis functions and analytical formulas for singular integrals [13] are applied. By high-order basis functions we can achieve better accuracy with a lower number of unknowns than by piecewise constant basis functions. In addition, the accuracy can be further increased by using nonuniform meshing with refinements on the areas where the potential varies most strongly, especially at the corners of the surfaces.

The results of polarizabilities of polyhedral inclusions can be applied in the analysis of dielectric mixing formulas, homogenization of heterogeneous media, and modeling of composite materials. Also it is important to remember that the results are applicable not only in electrostatic and electromagnetic modeling but also in other fields of physics [14] which involve quantities obeying the Laplace equation, like thermal conduction, diffusion, elasticity, and problems dealing with particle fluxes driven by chemical potentials.

## II. CALCULATION OF THE POLARIZABILITIES

### A. Integral Equation Formulation for the Potential Problem

The determination of the polarizability of an inclusion requires solving the electrostatic problem where the inclusion is located in a uniform external field  $\mathbf{E}_e$  according to Fig. 1.

The unknown potential, both inside and outside the inclusion, satisfies the Laplace equation

$$\nabla^2 \phi(\mathbf{r}) = 0. \quad (3)$$

Furthermore, far away from the scatterer the potential approaches the incident potential, which is the linear potential that gives rise to a uniform field:

$$\lim_{|\mathbf{r}| \rightarrow \infty} \phi(\mathbf{r}) = \phi_e(\mathbf{r}) = -E_e z. \quad (4)$$

Here, it has been assumed that the incident field is  $z$ -directed:  $\mathbf{E}_e = \mathbf{u}_z E_e$ . In the region external to the inclusion, the total potential  $\phi$  is a sum of the incident potential  $\phi_e$  and a ‘‘scattered’’ potential. This perturbational potential, the scattered potential, decays algebraically far away from the inclusion. It can be expanded into multipole series, and the strongest term of this series is the static dipole contribution to the potential. This term decays according to  $r^{-2}$ , and the corresponding field then obeys the law  $r^{-3}$ . Higher order multipoles give rise to potentials with higher powers of the distance in the denominator [1].

The dipole moment  $\mathbf{p}$  induced in the scatterer can be identified with the source of the dipolar component in the scattered field, and it is proportional to  $E_e$ . The ratio between these two,

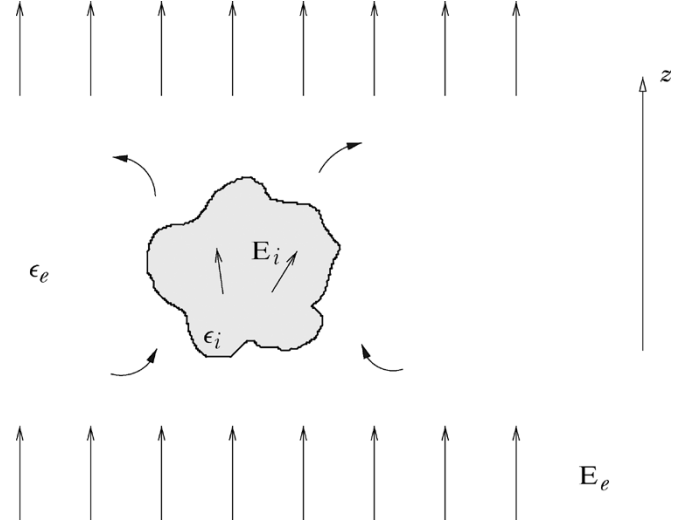


Fig. 1. Dielectric inclusion embedded in a uniform incident field  $\mathbf{E}_e$ . Note that the resulting internal field is not necessarily uniform. Also, close to the inclusion the external field is suffering a perturbation from the uniform distribution.

the induced dipole moment and the external field, gives us the polarizability as stated in (1).

An integral equation for the unknown potential function on the surface of the inclusion  $\phi$  in this electrostatic problem reads as follows [15]:

$$\phi_e(\mathbf{r}) = \frac{\tau+1}{2} \phi(\mathbf{r}) + \frac{\tau-1}{4\pi} \int_S \phi(\mathbf{r}') \frac{\partial}{\partial n'} \left( \frac{1}{|\mathbf{r}-\mathbf{r}'|} \right) dS', \quad \mathbf{r} \text{ on } S. \quad (5)$$

In this equation,  $S$  is the surface of the inclusion,  $\phi_e = -E_e z$  is the potential of the incident field, and  $\phi$  is the total potential on the surface.<sup>1</sup> The ratio of the permittivities is denoted by  $\tau = \epsilon_i/\epsilon_e$ , where  $\epsilon_i$  is permittivity of the inclusion. The outward normal to the surface is  $\mathbf{n}'$  at point  $\mathbf{r}'$ .

Equation (5) is a Fredholm integral equation of second kind. The integration has to be performed over the surface of the inclusion, and one might expect numerical difficulties when the integration point  $\mathbf{r}'$  and the field point  $\mathbf{r}$  coincide.

However, in the following we are dealing with polyhedra which have planar faces. This fact helps us to avoid the singularities to a certain extent because

$$\frac{\partial}{\partial n'} \left( \frac{1}{|\mathbf{r}-\mathbf{r}'|} \right) = \mathbf{n}' \cdot \nabla' \frac{1}{|\mathbf{r}-\mathbf{r}'|} = \mathbf{n}' \cdot \frac{\mathbf{r}-\mathbf{r}'}{|\mathbf{r}-\mathbf{r}'|^3} = 0 \quad (6)$$

if  $\mathbf{r}$  and  $\mathbf{r}'$  are located on the same face of the polyhedron. Indeed, the contribution to the integral vanishes over the whole face where the field point is located because of the vectors in the scalar product in (6) are orthogonal ( $\mathbf{n}'$  normal and the gradient tangential to the surface). So, fortunately, the singularity  $\mathbf{r} = \mathbf{r}'$  is automatically excluded. However, if the points  $\mathbf{r}$  and  $\mathbf{r}'$  are, for example, on adjacent faces of a polyhedron which are not in the same plane, the scalar product  $\mathbf{n}' \cdot (\mathbf{r}-\mathbf{r}')$  does not vanish. In that case the kernel  $K(\mathbf{r}, \mathbf{r}') = \partial/\partial n'(1/|\mathbf{r}-\mathbf{r}'|)$  is a singular function. Hence, special attention should be put to the numerical evaluation of the integrals near the corners when the

<sup>1</sup>Note that this is a 3-D problem which means that the kernel is of type  $1/r$ . For 2-D problems, the Green function would be logarithmic.

distance  $|\mathbf{r} - \mathbf{r}'|$  is small. Especially this will be the case on the edges and vertices of the regular polyhedra considered in this paper.

Once the potential is known on the surface, the dipole moment  $\mathbf{p}$  can be calculated from the polarization density  $\mathbf{P}$  of the inclusion

$$\mathbf{p} = \int_V \mathbf{P} dV = (\epsilon_i - \epsilon_e) \int_V \mathbf{E}_i dV = -(\epsilon_i - \epsilon_e) \int_V \nabla \phi(\mathbf{r}) dV \quad (7)$$

which can be transformed from the volume integral into a surface integral using Gauss's identity

$$\mathbf{p} = -(\tau - 1)\epsilon_e \int_S \phi(\mathbf{r}) \mathbf{n} dS. \quad (8)$$

In the above expressions,  $V$  is volume of the inclusion,  $\mathbf{E}_i$  is electric field within the inclusion and  $\mathbf{n}$  is the outward unit normal vector to  $S$ . Finally, the polarizability  $\alpha$  can be calculated from (1) using the known value for the dipole moment.

### B. Numerical Evaluation of the Potential

The potential function that is needed in the estimation of the polarizability can be calculated by integral equation (5). The earlier calculations in the literature are based on piecewise constant approximations for the potential (see, e.g., [6]). To improve the accuracy in this paper the unknown potential  $\phi$  is expressed by higher order basis functions. Let us suppose that the surface  $S$  is divided into planar triangular elements. Then we represent the unknown potential by a linear combination of basis functions  $u_n^{(q)}$  defined on these elements as

$$\phi = \sum_{n=1}^N c_n u_n^{(q)}. \quad (9)$$

Here,  $q = 1, 2, \dots$ , is the order of a basis function. For example, the third-order shape functions can be defined on a plane triangle as ([18] p. 2.125)

$$\begin{aligned} N_1^{(3)} &= \frac{1}{2}(3N_1 - 1)(3N_1 - 2)N_1 \\ N_2^{(3)} &= \frac{9}{2}N_1N_2(3N_1 - 1) \\ N_3^{(3)} &= \frac{9}{2}N_1N_2(3N_2 - 1) \\ N_4^{(3)} &= \frac{1}{2}(3N_2 - 1)(3N_2 - 2)N_2 \\ N_5^{(3)} &= \frac{9}{2}N_2N_3(3N_2 - 1) \\ N_6^{(3)} &= \frac{9}{2}N_3N_2(3N_3 - 1) \\ N_7^{(3)} &= \frac{1}{2}(3N_3 - 1)(3N_3 - 2)N_3 \\ N_8^{(3)} &= \frac{9}{2}N_1N_3(3N_3 - 1) \\ N_9^{(3)} &= \frac{9}{2}N_3N_1(3N_1 - 1) \\ N_{10}^{(3)} &= 27N_1N_2N_3 \end{aligned} \quad (10)$$

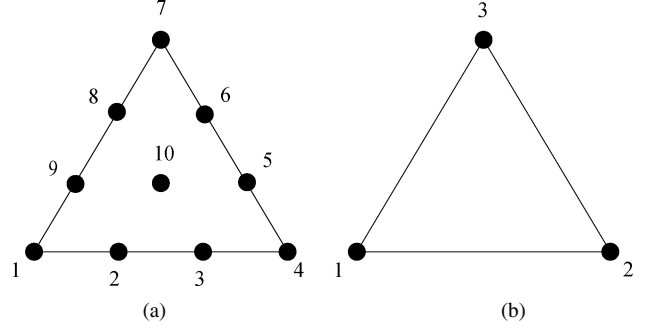


Fig. 2. (a) Nodes corresponding to the third-order and (b) linear-shape functions of a triangle.

where  $N_i = N_i^{(1)}$ ,  $i = 1, \dots, 3$ , are the standard linear shape functions. The corresponding node points are shown in Fig. 2. The basis functions are assembled from these shape functions so that they form continuous functions across the element boundaries.

Next we substitute representation (9) into (5). The resulting discretized equations are multiplied by test functions  $v_m^{(p)}$ ,  $m = 1, \dots, M$ , and integrated over  $S$ . This leads to the following matrix equation:

$$Ac = b. \quad (11)$$

Here  $c = [c_1, \dots, c_N]^T$  is the unknown coefficient vector and the elements of  $A$  and  $b$  are given by

$$A_{mn} = \int_{S'_m} v_m^{(p)}(\mathbf{r}) \left( \frac{\tau + 1}{2} u_n^{(q)}(\mathbf{r}) + \frac{\tau - 1}{4\pi} \times \int_{S_n} K(\mathbf{r}, \mathbf{r}') u_n^{(q)}(\mathbf{r}') dS' \right) dS \quad (12)$$

$$b_m = \int_{S'_m} v_m^{(p)}(\mathbf{r}) \phi_e(\mathbf{r}) dS \quad (13)$$

where  $S_n$  is the support of  $u_n^{(q)}$ ,  $S'_m$  is the support of  $v_m^{(p)}$  and the kernel  $K(\mathbf{r}, \mathbf{r}') = \partial/\partial n' (1/|\mathbf{r} - \mathbf{r}'|)$ . We apply Galerkin's method and choose  $v_m^{(p)} = u_m^{(q)}$  for all  $m$  and hence  $S'_m = S_m$ . Thereafter, matrix equation (11) is solved iteratively by the restarted version of the GMRES method [16].

Let us next consider numerical evaluation of the matrix elements (12) which include function  $K$  in the case where the distance  $|\mathbf{r} - \mathbf{r}'|$  is small. Evaluation of the other terms and evaluation of the elements (12) including  $K$  for large distances can be easily done by standard numerical techniques (see, e.g., [17]). Since the basis and test functions are expressed by polynomial nodal shape functions  $N^{(q)}$  of a (plane) triangle, it is sufficient to consider the following double integral:

$$\int_{T_m} N_m^{(q)}(\mathbf{r}) \int_{T_n} \frac{\partial}{\partial n'} \left( \frac{1}{|\mathbf{r} - \mathbf{r}'|} \right) N_n^{(q)}(\mathbf{r}') dS' dS. \quad (14)$$

Here,  $T_n$  and  $T_m$  are plane triangles on  $S$  so that  $N_n^{(q)}$  is a nodal shape function of  $T_n$  and  $N_m^{(q)}$  is a nodal shape function of  $T_m$ , respectively.

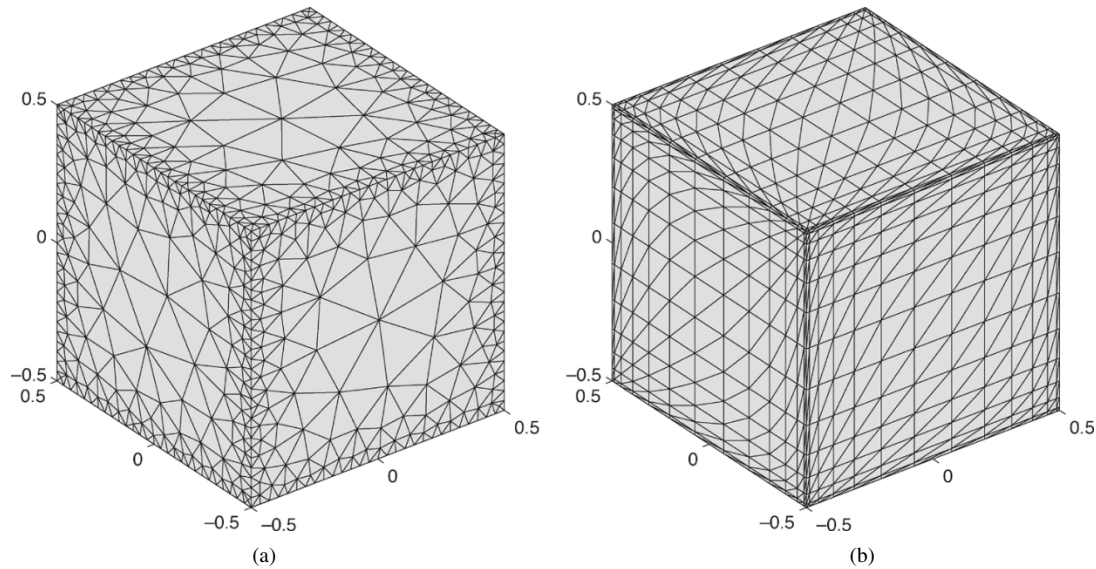


Fig. 3. Triangular meshes of a cube with (a) a linear and (b) square-root refinement on the edges.

First we calculate integral (14) with respect to  $\mathbf{r}'$  in closed form. Graglia [19] presented closed form formulas for integrals

$$\int_{T_n} \frac{\partial}{\partial n'} \left( \frac{1}{|\mathbf{r} - \mathbf{r}'|} \right) N_n^{(q)}(\mathbf{r}') dS' \quad (15)$$

with scalar and linear basis functions, i.e., for the cases  $q = 0$  and  $q = 1$ . Actually for  $q = 0$  integral (15) represents the solid angle in which a triangle  $T_n$  is seen at point  $\mathbf{r}$ . For the higher order basis functions,  $q \geq 2$ , the closed form formulas are presented in [13]. Because the kernel  $K$  is a singular function if  $\mathbf{r}$  is not on the same plane as the integration point is located, an application of the closed-form formulas will significantly increase the accuracy of calculation of (15).

After calculating integral (14) with respect to  $\mathbf{r}'$  in closed form the remaining integral with respect to  $\mathbf{r}$  is nonsingular. Thus, calculation of integral (14) with respect to  $\mathbf{r}$  can be performed by standard numerical techniques like Gaussian quadrature. If  $T_n$  and  $T_m$  are close to each other, more integration points should be applied.

In addition, since the potential  $\phi$  varies strongly near the corners of  $S$  [6], we have applied nonuniform meshing with linear or square root refinement near the corners. Examples of these meshes for a cube are displayed in Fig. 3. The numerical examples demonstrate that the analytical integration formulas combined with a nonuniform meshing and high-order basis functions ( $q = 3$ ) lead to results with a high accuracy. On the other hand, nonuniform meshing is not as crucial for “smooth” objects like dodecahedron or icosahedron as it is for a cube and tetrahedron which have sharper corners.

### III. NUMERICAL RESULTS

The results were calculated using a PC machine equipped with AMD XP 2000+ processor and 1024 Mbytes of RAM. The potential in connection with each polyhedron was solved for 123 different values of permittivity. For meshing density containing around 2000 elements and 9000 . . . 10 000 unknowns with third-order basis functions, the solution of a single case

of permittivity and the consequent calculation of the polarizability took typically 500 . . . 1000 seconds of computing time, depending on the value of  $\tau$  and other parameters.

The calculation time and accuracy depend on many factors, such as

- the number of elements;
- the order of basis functions;
- numerical integration;
- refinement of the mesh;
- stopping criterion of GMRES.


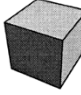



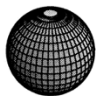
Since the singular part of the integral is calculated in closed form, numerical integration can be performed with a reasonable accuracy by taking enough integration points.

The critical factor seems to be the number of unknowns, which is limited by the finite sized computer memory. A better accuracy can be obtained without increasing the number of unknowns by using higher order basis functions and by focusing the unknowns to the areas where the potential has the strongest variation.

We tried both second- and third-order basis functions, and the third-order ones seem to give clearly better results. An appropriate refinement of the mesh, which takes into account the behavior of the potential at the edges and vertices, can also increase the accuracy. However, it is not clear what is an optimal refinement, since the potential is approximated by third-order polynomial basis functions. Although the scope of this paper was not meshing in particular, we made some experiments on the mesh refinements with the cube. Fig. 3 shows a mesh with a linear refinement on the edges so that the triangles keep their shape as regular as possible. Fig. 3 shows also another mesh with a square root refinement, where the refinement is applied only toward the edges. This gives more irregularly shaped triangles. However, numerical experiments show that the latter mesh gives better results.

We also applied other types of refinements, namely logarithmic and meshes where the meshing density behaves as  $d^{1/3}$  and  $d^{2/3}$ . Here,  $d$  is the distance from the edge. But, in most cases, the square root refinement (i.e.,  $d^{1/2}$ ) seems to produce

TABLE I  
LIMITING VALUES ( $\tau \rightarrow \infty$  AND  $\tau \rightarrow 0$ ) FOR THE NORMALIZED POLARIZABILITIES  $\alpha_n = \alpha/(\epsilon_e V)$  OF REGULAR POLYHEDRA. BEST NUMERICAL RESULTS ACCORDING TO THE PRESENT STUDY. THE ACCURACY IS SUCH THAT THE LAST SIGNIFICANT DIGIT IN THE RESULTS FOR POLYHEDRA SHOULD BE CORRECT TO  $\pm 1$ , EXCEPT FOR TETRAHEDRON IN WHICH CASE IT IS  $\pm 5$

	<i>polyhedron</i>	$\alpha_n(\tau \rightarrow \infty)$	$\alpha_n(\tau \rightarrow 0)$
	tetrahedron	5.0285	-1.8063
	hexahedron	3.6442	-1.6383
	octahedron	3.5507	-1.5871
	dodecahedron	3.1779	-1.5422
	icosahedron	3.1304	-1.5236
	sphere	3.0002	-1.5000

best results. Similar systematic study has not been carried out in the case of the other polyhedra. The results of Table I are obtained by calculating the polarizabilities with a uniform mesh and with a square root refinement. By repeating the calculations for a couple of various meshing densities, we have concluded the results of Table I.

The stopping criterion for the GMRES method is

$$\frac{\|Ac - b\|_2}{\|b\|_2} < tol \quad (16)$$

where *tol* is a given error tolerance. We tried  $tol = 10^{-6}$ ,  $10^{-8}$ , and  $10^{-12}$ . The value  $10^{-8}$  seems to give sufficient accuracy and in that case the error is generated by other factors than the iterative solver.

The results of our calculations for the polarizabilities of the various polyhedra are shown in Fig. 4 and normalized to the sphere value in Fig. 5. Also, Table I lists the limiting values for the five enumerated polarizabilities when the permittivity ratio approaches either zero or infinity. We are plotting the nor-

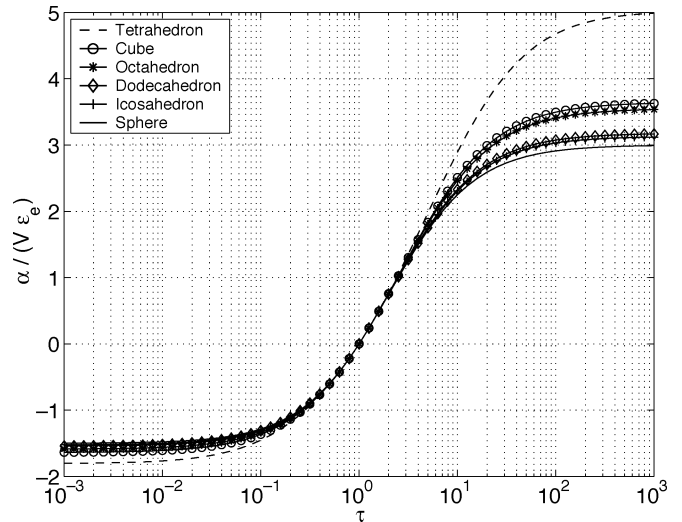


Fig. 4. Normalized polarizabilities of the five Platonic solids as functions of the permittivity. The polarizability of sphere is also shown. Note the similarity between icosahedron and dodecahedron, and also the similarity between cube and octahedron. The clearly highest curve belongs to tetrahedron.

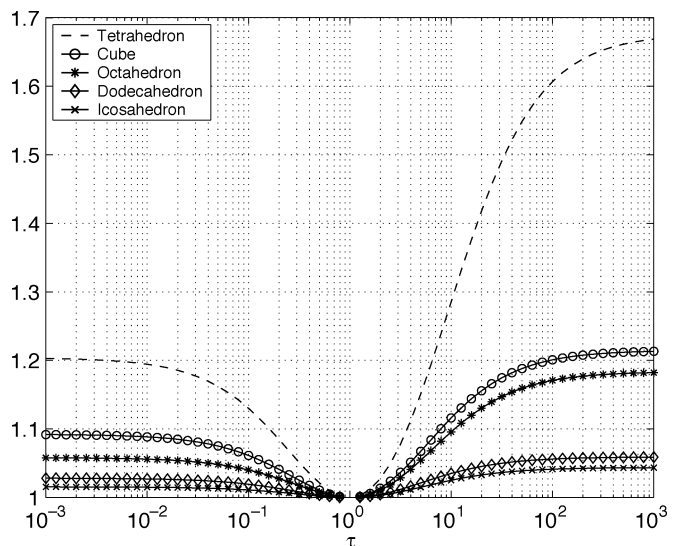


Fig. 5. Polarizabilities of the five Platonic solids as functions of the permittivity as in Fig. 4, normalized to the polarizability of a sphere with the same volume and permittivity.

malized polarizability defined by  $\alpha_n = \alpha/(\epsilon_e V)$ , which for a sphere has a simple form

$$\alpha_n = \frac{\alpha}{\epsilon_e V} = 3 \frac{\tau - 1}{\tau + 2}. \quad (17)$$

Fig. 6 compares the results with those found out by other researchers. In the literature, results can be found for the cube, especially for the limiting case of the polarizability of the cube with infinite permittivity. It can be seen that the accuracy of the results has increased considerably along with the results from the two latest years.

What can we say about how close the calculated results for the polarizability are to the correct values? An indication for the accuracy comes from the way the increase in the number of unknowns and increasing the meshing density affects the polarizability results. The worst case (producing least accurate results)

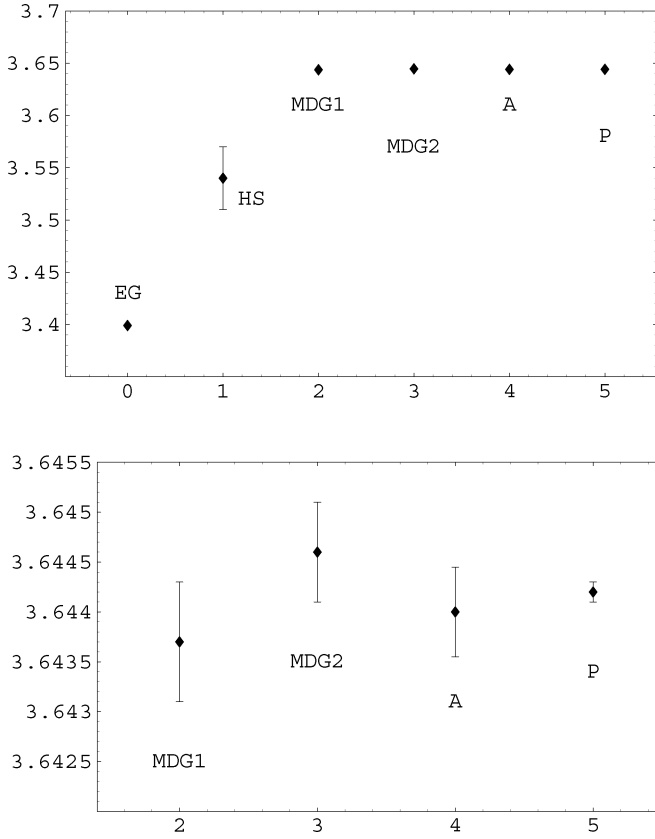


Fig. 6. Comparison of the results for the normalized polarizability  $\alpha_n$  of a cube with permittivity approaching infinity. Earlier results: EG [5], HS [4], MDG [8], A [6], [7]. The present work is marked by P. The lower graph is a magnification of the upper one.

is clearly the case of infinite permittivity of the scatterer. From series of calculations we could estimate that the worst-case inaccuracy is around  $5 \cdot 10^{-4}$  for tetrahedra and  $10^{-4}$  for icosahedra, in absolute terms.

Another implication for the accuracy of the results can be measured by calculating the well-known polarizability of a sphere with the same code. With 9000 unknowns, the polarizability emerges with accuracy  $2 \cdot 10^{-4}$  for the worst case.<sup>2</sup> Of course, one should be careful with identifying the reason and quantity of this inaccuracy with the polyhedral results: firstly, the sphere is more difficult to model with finite planar surface elements due to its curved surface, but on the other hand, the sphere behaves electrically in an “easier” manner because it does not have corners.

#### IV. INTERPOLATION FORMULAS

In the following, formulas are given with which accurate estimates for the polarizabilities of Platonic solids can be made as

<sup>2</sup>This means that for infinite permittivity the normalized polarizability is overestimated to be 3.0002.

<sup>3</sup>The website of the Electromagnetics Laboratory of HUT contains a Java applet with which anybody can calculate the Platonic polarizabilities according to the interpolation formulas: <http://www.hut.fi/Yksikot/Sahkomagnetiikka/kurssit/animaatio/Polarisaatio.html>

functions of the permittivity contrast.<sup>3</sup> A rather satisfactory fit with the calculated data results from the use of Padé approximations as functions of the permittivity ratio  $\tau$ . In the optimization of the coefficients in these interpolation formulas, *a priori* knowledge of the polarizabilities was included. It can be inferred from [20], [21] that if we use the variable

$$\kappa = \frac{\tau - 1}{\tau + 2} = \frac{\epsilon_i - \epsilon_e}{\epsilon_i + 2\epsilon_e} \quad (18)$$

in the expansion of the polarizability, it behaves as

$$\alpha_n = 3\kappa + a_3\kappa^3 + a_4\kappa^4 + \dots \quad (19)$$

For example, for a sphere the normalized polarizability is  $\alpha_n = 3\kappa$ .

Note, however, that the Taylor series in terms of  $\kappa$  converge quite slowly, and therefore, in calculations that make use of the following results, the Padé approximation should be used.

##### A. Tetrahedron

$$\alpha_n \approx \alpha_\infty(\tau - 1) \frac{\tau^3 + 7.65667\tau^2 + 8.50919\tau - \alpha_0}{\tau^4 + 14.1983\tau^3 + 44.9182\tau^2 + 30.2668\tau + \alpha_\infty} \quad (20)$$

where  $\alpha_\infty = 5.0285$  and  $\alpha_0 = -1.8063$ .

A Taylor expansion of this approximation in terms of  $\kappa$  gives

$$\alpha_n \approx 3\kappa + 1.42812\kappa^3 - 0.64265\kappa^4 + 1.25207\kappa^5 - 1.03851\kappa^6 + 1.52913\kappa^7 - 1.69626\kappa^8 \quad (21)$$

##### B. Cube

$$\alpha_n \approx \alpha_\infty(\tau - 1) \frac{\tau^3 + 4.83981\tau^2 + 5.54742\tau - \alpha_0}{\tau^4 + 8.0341\tau^3 + 19.3534\tau^2 + 15.4349\tau + \alpha_\infty} \quad (22)$$

where  $\alpha_\infty = 3.6442$  and  $\alpha_0 = -1.6383$ .

Taylor expansion of this approximation in terms of  $\kappa$

$$\alpha_n \approx 3\kappa + 0.71355\kappa^3 - 0.34804\kappa^4 + 0.45065\kappa^5 - 0.39060\kappa^6 + 0.42727\kappa^7 - 0.44059\kappa^8. \quad (23)$$

##### C. Octahedron

$$\alpha_n \approx \alpha_\infty(\tau - 1) \frac{\tau^3 + 5.13936\tau^2 + 5.86506\tau - \alpha_0}{\tau^4 + 8.26227\tau^3 + 19.8267\tau^2 + 15.6191\tau + \alpha_\infty} \quad (24)$$

where  $\alpha_\infty = 3.5507$  and  $\alpha_0 = -1.5871$ .

Taylor expansion of this approximation in terms of  $\kappa$

$$\alpha_n \approx 3\kappa + 0.52836\kappa^3 - 0.15702\kappa^4 + 0.22333\kappa^5 - 0.13073\kappa^6 + 0.14303\kappa^7 - 0.12520\kappa^8. \quad (25)$$

### D. Dodecahedron

$$\alpha_n \approx \alpha_\infty (\tau - 1) \frac{\tau^2 + 2.421\,01\tau - \frac{2.568\,42\alpha_0}{\alpha_\infty}}{\tau^3 + 4.729\,32\tau^2 + 6.534\,64\tau + 2.568\,42} \quad (26)$$

where  $\alpha_\infty = 3.1779$  and  $\alpha_0 = -1.5422$ .

Taylor expansion of this approximation in terms of  $\kappa$

$$\alpha_n \approx 3\kappa + 0.239\,47\kappa^3 - 0.117\,31\kappa^4 + 0.097\,089\kappa^5 - 0.074\,184\kappa^6. \quad (27)$$

### E. Icosahedron

$$\alpha_n \approx \alpha_\infty (\tau - 1) \frac{\tau^2 + 3.049\,68\tau - \frac{4.0896\alpha_0}{\alpha_\infty}}{\tau^3 + 5.291\,69\tau^2 + 8.526\,87\tau + 4.0896} \quad (28)$$

where  $\alpha_\infty = 3.1304$  and  $\alpha_0 = -1.5236$ .

Taylor expansion of this approximation in terms of  $\kappa$

$$\alpha_n \approx 3\kappa + 0.154\,06\kappa^3 - 0.046\,122\,7\kappa^4 + 0.034\,121\kappa^5 - 0.018\,884\kappa^6. \quad (29)$$

## V. DISCUSSION

A comparison of the polarizabilities of the various polyhedra (for example, Fig. 4 or Table I) shows that in terms of magnitude, the polarizabilities fall in obvious order:

- sphere;
- icosahedron;
- dodecahedron;
- octahedron;
- cube;
- tetrahedron.

Given a volume and permittivity, the sphere has the lowest value. This minimum behavior of the sphere is a well-known phenomenon. Then the polarizability order follows the number of faces of the polyhedron, with icosahedron being closest to the sphere, and tetrahedron having the highest polarizability. This sounds reasonable because tetrahedron has the sharpest corners of these objects, and one could expect that charge is concentrated there, leading to a strong integrated dipole moment.

But we can also see from Fig. 4 that the number of faces does not fully correlate with the magnitude of the polarizability. In terms of polarizabilities, cube and octahedron resemble each other, and so also do the dodecahedron and the icosahedron, despite their clear differences as to the number of faces.

Table II shows the various geometrical parameters of the five solids. It can be seen that the number of faces is not the best estimator for the polarizability of the polyhedron. Stronger correlation exists between the polarizability on one hand and on the other, either the number of edges, or the solid angle subtended by the adjacent faces. A tetrahedron has the sharpest vertex (its solid angle is the smallest of all

TABLE II  
GEOMETRIC CHARACTERISTICS OF POLYHEDRA

polyhedron	faces	edges	vertices	solid angle seen from the vertex
tetrahedron	4	6	4	0.55129
hexahedron	6	12	8	$\pi/2 \approx 1.5708$
octahedron	8	12	6	1.3593
dodecahedron	12	30	20	2.9617
icosahedron	20	30	12	2.6345

five). As a side note, it is interesting that the number of faces and the sharpness of vertices increase differently from one polyhedron to another: an octahedron has sharper vertices than the cube, and also the vertex of an icosahedron is sharper than that of a dodecahedron.

The number of edges seems to a good indicator of the polarizability: tetrahedron (4 edges) has the highest polarizability, cube and octahedron (12 edges) are in the middle, and dodecahedron and icosahedron (30 edges) are closest to the minimum which is the polarizability of a sphere.

There remains the question of isotropy of the polarizability of the inclusions. Does the dipole moment response depend on the orientation of the polyhedron with respect to the electric field? It is obvious that for a sphere, there is no special direction in the geometry, and hence the polarizability is also a scalar. Platonic polyhedra display less symmetry than a sphere, but nevertheless, the remaining symmetry for each polyhedron is sufficient to degenerate the dyadic relation between the dipole moment and the external field  $\mathbf{p} = \bar{\alpha} \cdot \mathbf{E}_e$  into a simpler one,  $\mathbf{p} = \alpha \mathbf{E}_e$ , with a scalar polarizability. This fact can be appreciated with the following reasoning: the polarizability relation is described by a real and symmetric matrix in the lossless and reciprocal case we are considering. Therefore, its eigenvectors are orthogonal and eigenvalues real [22, p. 195]. If the polarizability of a polyhedron were not a multiple of a unit dyadic (meaning that the three eigenvalues were not equal), there should be particular direction which originates from the shape of the inclusion. But this is forbidden by the symmetry of the geometrical structure. This kind of reasoning can be used to motivate the treatment of the polarizabilities in this paper as *a priori* scalars.

## ACKNOWLEDGMENT

The authors would like to express their thanks to M. Taskinen for his kind assistance in connection with the meshing of the scatterers as well as with the properties of regular polyhedra. Also the comments by the Reviewers were helpful.

## REFERENCES

- [1] J. D. Jackson, *Classical Electrodynamics*, 3rd ed. New York: Wiley, 1999.
- [2] A. Sihvola, *Electromagnetic Mixing Formulas and Applications*, ser. Electromagnetic Wave Series 47. London, U.K.: IEE Publishing, 1999.
- [3] T. W. Edwards and J. Van Bladel, "Electrostatic dipole moment of a dielectric cube," *Appl. Sci. Res.*, vol. 9B, pp. 151–155, 1961.
- [4] D. F. Herrick and T. A. Senior, "The dipole moment of a dielectric cube," *IEEE Trans. Antennas Propagat.*, vol. AP-25, pp. 590–592, July 1977.

- [5] L. Eyges and P. Gianino, "Polarizabilities of rectangular dielectric cylinders and of a cube," *IEEE Trans. Antennas Propagat.*, vol. AP-27, pp. 557–560, July 1979.
- [6] J. Avelin, R. Sharma, I. Hänninen, and A. H. Sihvola, "Polarizability analysis of cubical and square-shaped dielectric scatterers," *IEEE Trans. Antennas Propagat.*, vol. 49, pp. 451–457, Mar. 2001.
- [7] J. Avelin and A. Sihvola, "Polarizability of polyhedral dielectric scatterers," *Microwave Opt. Technol. Lett.*, vol. 32, no. 1, pp. 60–64, 2002.
- [8] M. L. Mansfield, J. F. Douglas, and E. J. Garboczi, "Intrinsic viscosity and the electrical polarizability of arbitrarily shaped objects," *Phys. Rev. E, Stat. Phys. Plasmas Fluids Relat. Interdiscip. Top.*, vol. 64, no. 6, pp. 61 401–61 416, December 2001.
- [9] B. Sareni, L. Krähenbühl, A. Beroual, and C. Brosseau, "Effective dielectric constant of periodic composite materials," *J. Appl. Phys.*, vol. 80, no. 3, pp. 1688–1696, Aug. 1, 1996.
- [10] B. Sareni, L. Krähenbühl, A. Beroual, A. Nicolas, and C. Brosseau, "A boundary integral equation method for the calculation of the effective permittivity of periodic composites," *IEEE Trans. Magn.*, vol. 33, pp. 1580–1583, Mar. 1997.
- [11] F. Wu and K. W. Whites, "Quasistatic effective permittivity of periodic composites containing complex shaped dielectric particles," *IEEE Trans. Antennas Propagat.*, vol. 49, pp. 1174–1182, Aug. 2001.
- [12] K. W. Whites and F. Wu, "Effects of particle shape on the effective permittivity of composite materials with measurements for lattices of cubes," *IEEE Trans. Microwave Theory Tech.*, vol. 50, pp. 1723–1729, July 2002.
- [13] S. Järvenpää, M. Taskinen, and P. Ylä-Oijala, "Singularity extraction technique for integral equation methods with higher order basis functions on plane triangles and tetrahedra," *Int. J. Numer. Methods Eng.*, vol. 58, pp. 1149–1165, 2003.
- [14] G. W. Milton, *The Theory of Composites*. Cambridge, U.K.: Cambridge Univ. Press, 2002.
- [15] J. Van Bladel, *Electromagnetic Fields*, revised ed. New York: Hemisphere, 1985.
- [16] Y. Saad and M. H. Schultz, "GMRES: a generalized minimal residual algorithm for solving nonsymmetric linear systems," *SIAM J. Sci. Stat. Comput.*, vol. 7, pp. 856–869, 1986.
- [17] D. A. Dunavant, "High degree efficient symmetrical Gaussian quadrature rules for the triangle," *Int. J. Numerical Methods Eng.*, vol. 21, pp. 1129–1148, 1985.
- [18] *Finite Element Handbook*, H. Kardestuncer and D. H. Norrie, Eds., McGraw-Hill, New York, 1987.
- [19] R. D. Graglia, "On the numerical integration of the linear shape functions times the 3-D Green's function or its gradient on a plane triangle," *IEEE Trans. Antennas Propagat.*, vol. 41, pp. 1448–1455, 1993.
- [20] S. Torquato, "Effective electrical conductivity of two-phase disordered composite media," *J. Appl. Phys.*, vol. 58, no. 10, pp. 3790–3797, November 1985.
- [21] E. J. Garboczi and J. F. Douglas, "Intrinsic conductivity of objects having arbitrary shape and conductivity," *Phys. Rev. E*, vol. 53, no. 6, pp. 6169–6180, June 1996.
- [22] G. Arfken, *Mathematical Methods for Physicists*, 2nd ed. New York: Academic Press, 1970.



**Ari Sihvola** (S'80–M'86–SM'91) was born on October 6, 1957, in Valkeala, Finland. He received the degrees of Diploma Engineer, Licentiate of Technology, and Doctor of Technology, all in electrical engineering, from the Helsinki University of Technology (HUT), Espoo, Finland, in 1981, 1984, and 1987, respectively.

Besides working for HUT and the Academy of Finland, he was a Visiting Engineer in the Research Laboratory of Electronics, Massachusetts Institute of Technology, Cambridge, from 1985 to 1986, and a Visiting Scientist at the Pennsylvania State University, State College, from 1990 to 1991. He was a Visiting Scientist at Lund University, Sweden, in 1996, and a Visiting Professor at the Electromagnetics and Acoustics Laboratory, Swiss Federal Institute of Technology, Lausanne, for the academic year 2000 to 2001. Currently, he is a Professor of electromagnetics at HUT with interest in electromagnetic theory, complex media, materials modeling, remote sensing, and radar applications.

Dr. Sihvola is Vice Chairman of the Finnish National Committee of the International Union of Radio Science (URSI). He also served as the Secretary of the 22nd European Microwave Conference, held in August 1992, in Espoo, Finland.

**Pasi Ylä-Oijala** received the M.Sc. and Ph.D. degrees in applied mathematics from the University of Helsinki, Helsinki, Finland, in 1992 and 1999, respectively.

Since October 2002, he has been working as a Researcher in the Electromagnetics Laboratory, Helsinki University of Technology, Espoo, Finland. His field of interest includes numerical techniques in computational electromagnetics based on the integral equation methods.

**Seppo Järvenpää** was born in 1965. He received the M.Sc. and Ph.D. degrees in applied mathematics from the University of Helsinki, Helsinki, Finland, in 1992 and 2001, respectively.

Currently he is working as a Researcher in the Electromagnetics Laboratory, Helsinki University of Technology, Espoo, Finland. His field of interest includes numerical techniques in computational electromagnetics based on finite element and integral equation methods.

**Juha Avelin** received the degree of Diploma Engineer in electrical engineering, from Helsinki University of Technology (HUT), Espoo, Finland, in 1999.

He is currently working as a Researcher in the Electromagnetics Laboratory of HUT. His current research interests are homogenization of mixtures and canonical problems in electromagnetics.